

DISCRETE AND DIFFUSE X-RAY EMISSION IN THE NUCLEUS AND DISK OF THE STARBURST SPIRAL GALAXY M83

R. Soria¹ and K. Wu¹

Mullard Space Science Laboratory, University College London, Holmbury St Mary, Surrey RH5 6NT, UK

ABSTRACT

We have studied the face-on, barred spiral M83 (NGC 5236) with *Chandra*. Eighty-one point sources are detected (above $3.5\text{-}\sigma$) in the ACIS S3 image: 15 of them are within the inner $16''$ region (starburst nucleus, resolved for the first time with *Chandra*), and 23 within the inner $60''$ (including the bar). The luminosity distributions of the sources in the inner $60''$ region (nucleus and stellar bar) is a single power law, which we interpret as due to continuous, ongoing star formation. Outside this inner region, there is a smaller fraction of bright sources, which we interpret as evidence of an aging population from a past episode of star formation. About 50% of the total emission in the nuclear region is unresolved; of this, about 70% can be attributed to hot thermal plasma, and we interpret the rest as due to unresolved point sources (eg, faint X-ray binaries). The unresolved X-ray emission also shows differences between the nuclear region and the spiral arms. In the nuclear region, the electron temperature of the thermal plasma is ≈ 0.58 keV. In the spiral arms, the thermal component is at $kT \approx 0.31$ keV and a power-law component dominates at energies $\gtrsim 1$ keV. The high abundance of C, Ne, Mg, Si and S with respect to Fe suggests that the interstellar medium is enriched and heated by core-collapse supernova explosions and winds from massive stars.

Key words: Galaxies: individual: M83 (=NGC 5236) – Galaxies: nuclei – Galaxies: spiral – Galaxies: starburst – X-rays: binaries – X-rays: galaxies

1. INTRODUCTION

M83 (NGC 5236) is a grand-design, barred spiral galaxy (Hubble type SAB(s)c) with a starburst nucleus. Distance estimates are still very uncertain. A value of 3.7 Mpc was obtained by de Vaucouleurs et al. (1991). This places the galaxy in the Centaurus A group, whose members have a large spread in morphology and high velocities, indicating that the group is not virialised and tidal interactions and merging are frequent (de Vaucouleurs 1979; Côté et al. 1998).

M83 was observed in the X-ray bands by *Einstein* in 1979–1981 (Trinchieri et al. 1985), by *ROSAT* in 1992–1994 (Immler et al. 1999), and by *ASCA* in 1994 (Okada

et al. 1997). Twenty-one point sources were found in the *ROSAT*/HRI image, but the starburst nuclear region was unresolved.

M83 was observed by *Chandra* on 2000 April 29, with the ACIS-S3 chip at the focus. The data became available to the public in mid-2001. The total exposure time was 50.978 ks; after screening out observational intervals corresponding to background flares, we retained a good time interval of 49.497 ks.

In this paper we present the luminosity distribution of the discrete source population and discuss the properties of the unresolved emission in the nuclear region and in the disk. For further details on the data analysis techniques, and for more extensive discussions on the properties of the individual sources, see Soria & Wu (2002).

2. GLOBAL PROPERTIES OF THE DISCRETE SOURCES

A total of 81 point sources are detected in the S3 chip at a $3.5\text{-}\sigma$ level in the 0.3–8.0 keV band. The source list is given in Soria & Wu (2002). Comparing the position of the *Chandra* S3 sources with a VLT *B* image shows that the off-centre sources tend to associate with the optically bright regions (Figure 1). The sources have a large spread in the hardness of their X-ray emission. A “true-colour” X-ray image of the nuclear region is shown in Figure 2, bottom panel.

Separating the sources inside and outside a circular region of radius $60''$ from the geometric centre of the X-ray emission reveals that the two groups have different luminosity distributions in the 0.3–8.0 keV band. (A linear separation of $60''$ corresponds to 1.1 kpc for a distance of 3.7 Mpc, and is roughly half of the total length of the major galactic bar.) The cumulative $\log N(>S) - \log S$ distribution (where S are the photon counts) of the sources inside this inner region can be described as a single power law, with a slope of -0.8 . The $\log N(>S) - \log S$ curve of the sources outside the circular inner region instead is neither a single nor a broken power law (Figure 3). It shows a kink at $S \approx 250$ cts; the slope of the curve above the kink is -1.3 , while it is -0.6 at the faint end. If we assume a foreground absorbing column density $n_{\text{H}} = 4 \times 10^{20} \text{ cm}^{-2}$ (Schlegel et al. 1998), a distance of 3.7 Mpc and a power-law spectrum with photon index $\Gamma = 1.5$ for all the sources, 100 counts ($\approx 2.0 \times 10^{-3} \text{ cts s}^{-1}$) correspond to an unabsorbed source luminosity $L_{\text{x}} = 2.3 \times 10^{37} \text{ erg s}^{-1}$

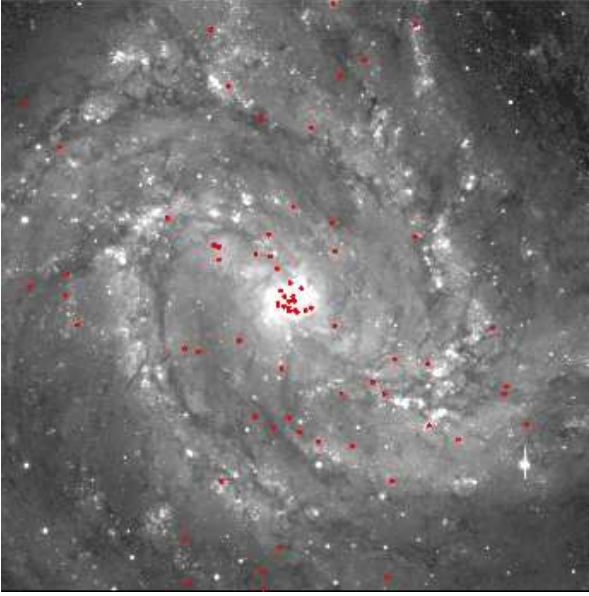


Figure 1. Spatial distribution of the discrete X-ray sources overplotted on a VLT B image (size: $6'.8 \times 6'.8$).

in the 0.3–8.0 keV band. The kink in the $\log N(>S) - \log S$ curve of the sources outside the $60''$ circle is therefore located at $L_x \approx 6 \times 10^{37} \text{ erg s}^{-1}$ (0.3–8.0 keV band).

We estimate from the Deep Field South survey (Giacconi et al. 2001) that about 15% of the 81 sources are background AGN; the expected number in the inner $60''$ circle is smaller than one. The kink in the $\log N(>S) - \log S$ curve for the outer sources and the values of the slope at both ends are unaffected by the background subtraction.

The flatter slope of the $\log N(>S) - \log S$ curve at the high-luminosity end for the population of sources in the inner $60''$ region implies a larger proportion of bright sources than in source population further away from the nucleus. The situation is different for example in the spiral galaxy M81, where most bright sources are found in the galactic disk instead of the nuclear region (Tennant et al. 2001). If the flatness of the slope in the $\log N(>S) - \log S$ curve is a characteristic of ongoing star formation (Wu 2001), the difference in the spatial distribution of the brightest sources in M83 and M81 is simply a consequence of the fact that M83 has a starburst nucleus while star formation in galaxies such as M81 is presently more efficient in the disk.

3. EMISSION FROM THE NUCLEAR REGION

The *Chandra* data reveal that M83 has a very highly structured nuclear region (Figure 2, bottom panel). Fifteen discrete sources are detected within a radius of $\approx 16''$ (≈ 290 pc) from the centre of symmetry of the outer optical isophotes. A spectral analysis of the two brightest sources is presented in Soria & Wu (2002), and an analysis of other point sources will be presented in Soria et al. (in prepara-

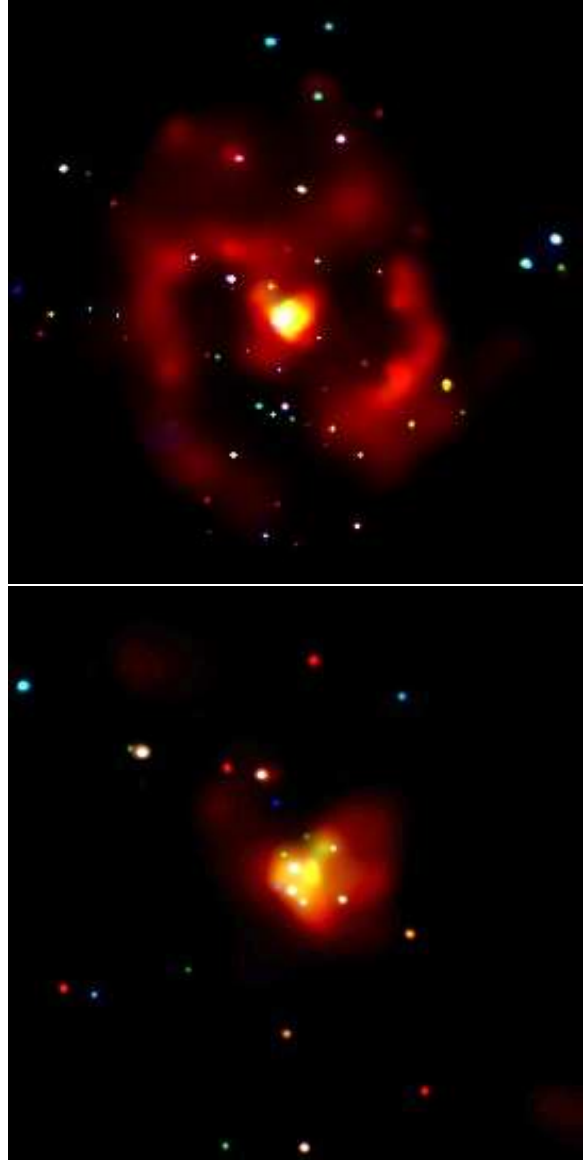


Figure 2. Top panel: A low-resolution (ACIS-S3 chip, with pixels binned 4×4) true-colour image of M83 shows strong unresolved emission both in the starburst nuclear region and along the spiral arms. Bottom panel: full-resolution true-colour image of the central region (size: $3' \times 3'$). In both images, red, green and blue correspond to emission in the 0.3–1.0 keV, 1.0–2.0 keV and 2.0–8.0 keV bands respectively. Both images have been adaptively smoothed.

tion). We removed the point sources and extracted counts from concentric annuli to construct radial brightness profiles of the unresolved emission in the nuclear region. We found that the brightness is approximately constant in a circular region up to a radius of $7''$ and then declines radially with a power-law like profile. The azimuthally-averaged profile is well fitted by a King profile, with a core radius of $6''.7 \pm 0''.5$ (≈ 120 pc), and a power law with a slope of -1.9 ± 0.2 beyond the core.

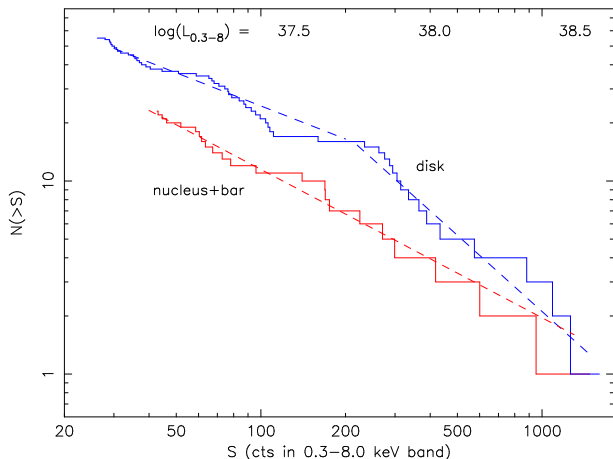


Figure 3. The cumulative luminosity distributions of sources found in the 0.3–8.0 keV band is different for the population inside the 60'' inner circle (which includes the starburst nuclear region and the main bar) and for the population outside of it (red and blue curves respectively). We interpret the single power-law distribution of the nuclear sources as evidence of continuous, ongoing star formation. The relative scarcity of bright sources in the disk population may be the effect of aging, which suggests that star formation is less active there. See Section 2 for the conversion from counts to luminosity.

We extracted the spectrum of the unresolved emission inside the inner 16'' circle, excluding the resolved point sources, and we fitted it using an absorbed, single-temperature vmekal plus power-law model. Assuming solar abundances, we obtain a best-fit electron temperature $kT = (0.60^{+0.02}_{-0.03})$ keV and a power-law photon index $\Gamma = 3.1^{+0.1}_{-0.2}$. The predicted lines are not strong enough to account for the data, leading to poor fit statistics ($\chi^2_\nu = 1.42$, 114 dof). Increasing the abundance of all the metals by the same constant factor does not improve the fit.

We then assumed a different set of abundances, higher than solar for C, Ne, Mg, Si and S, and slightly underabundant for Fe (see Table 1 in Soria & Wu 2002). This is physically justified if the interstellar medium has been enriched by type-II supernova ejecta and winds from very massive, young stars. We obtain a best-fit temperature $kT = (0.58^{+0.03}_{-0.02})$ keV, and power-law photon index $\Gamma = 2.7^{+0.3}_{-0.3}$ ($\chi^2_\nu = 0.99$, 114 dof).

We also estimated the total (resolved plus unresolved) luminosity from the circular regions within radii of 7'' (this is approximately the region inside the outer dust ring) and 16'' from the geometric centre of the X-ray emission, using an absorbed, optically-thin thermal plasma plus power-law model. The total emitted luminosity in the 0.3–8.0 keV band is $\approx 15.7 \times 10^{38}$ erg s $^{-1}$ inside 7'' and $\approx 23.8 \times 10^{38}$ erg s $^{-1}$ inside 16'' (Table 1). Discrete sources contribute $\approx 50\%$ of the total luminosity. The unresolved emission is itself the sum of truly diffuse emission from

Table 1. Luminosity of emission from discrete and unresolved sources in the nuclear region (0.3–8.0 keV band).

luminosity ($\times 10^{38}$ erg s $^{-1}$)	inside 7''	inside 16''
discrete sources	7.7	12.3
unresolved sources	8.0	11.5
optically-thin thermal component	5.5	7.8
power-law component	2.5	3.7
total	15.7	23.8

optically thin gas, and emission from unresolved point-like sources (eg, faint X-ray binaries). Assuming that the latter contribution is responsible for the power-law component in the spectrum of the unresolved emission, we estimate that emission from truly diffuse thermal plasma contributes $\approx 35\%$ of the total luminosity (Table 1).

Extrapolating the $\log N(>S) - \log S$ curve for the nuclear sources gives us another way of estimating the relative contribution to the unresolved emission of truly diffuse gas and faint point-like sources. We obtain that unresolved point-like X-ray sources inside 16'' would have a total luminosity of $\approx 2.7 \times 10^{38}$ erg s $^{-1}$ (see Soria & Wu 2002 for details). Another possible contribution to the unresolved emission comes from photons emitted by the resolved sources but falling outside the extraction regions, in the wings of the PSF. We estimate that this contribution is $\lesssim 1.5 \times 10^{38}$ erg s $^{-1}$. Thus, the combined contribution of faint X-ray sources and emission in the wings of the PSF can account for the luminosity of the power-law component inferred from the spectral fitting of the unresolved emission. This also confirms that a substantial proportion ($\approx 70\%$) of the unresolved emission is indeed due to truly diffuse gas rather than faint point-like sources.

Diffuse X-ray emission is also clearly observed along the spiral arms (Figure 2, top panel). We compared the spectrum of the unresolved emission in the nuclear region and along the arms, and found that the unresolved arm emission has a thermal component dominating at lower energies, and a power-law-like component, dominating above 1 keV. The thermal component in the arms has a temperature $T = 0.31^{+0.01}_{-0.03}$ keV, much cooler than that in the nucleus. The power-law component has a photon index $\Gamma = 1.42^{+0.08}_{-0.05}$. A more detailed analysis of the unresolved arm emission will be presented in Soria et al. (in preparation).

4. DISCUSSION

Separating the discrete sources inside and outside a 60'' central region reveals that the two populations have different

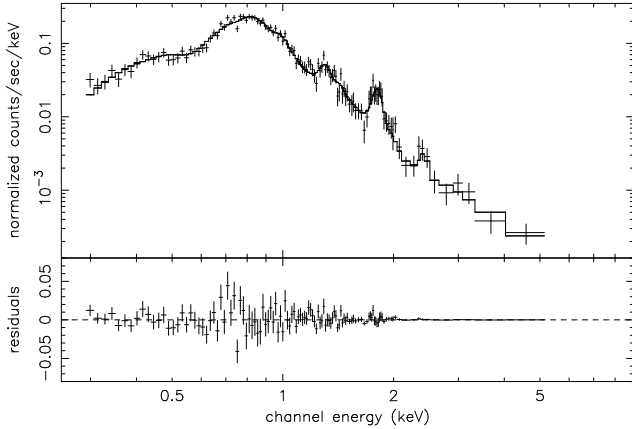


Figure 4. The spectrum of the unresolved emission in the nuclear region (inside a $16''$ circle) shows very strong emission lines from Mg XI (1.33–1.35 keV), Si XIII (1.84–1.87 keV) and SXV (2.43 keV). The other major contributions to the spectrum come from C VI (0.37–0.44 keV), O VII (triplet, 0.56–0.57 keV), Ne IX (triplet, 0.91–0.92 keV), Ne X (1.02 keV), and the Fe XVII L-line complex (0.6–0.9 keV).

cumulative luminosity distributions. The $\log N(>S) - \log S$ curve of the sources outside this radius (i.e., the disk population) shows a kink at a luminosity $\approx 6 \times 10^{37} \text{ erg s}^{-1}$ in the 0.3–8.0 keV band. No kink is seen for the sources inside the $60''$ radius (i.e., those located in the nuclear region and along the bar). The slope of the $\log N(>S) - \log S$ curve at its high-luminosity end is flatter for the nuclear population, implying a larger proportion of bright sources (possible black-hole candidates). We interpret this as evidence of a past star formation episode in the disk, while there is continuous, ongoing star formation in the nuclear region (Wu 2001).

About 50% of the total emission in the nuclear region belongs to resolved discrete sources. We estimate that $\approx 70\%$ of the unresolved emission (35% of the total) is due to truly diffuse plasma, with the rest (15% of the total) coming from faint, unresolved point-like sources and photons in the wings of the PSF outside the detection cells of the resolved sources.

The X-ray spectrum of the unresolved nuclear component shows strong emission lines, and can be modelled as emission from optically-thin thermal plasma at $kT \approx 0.6$ keV. Above-solar abundances of Ne, Mg, Si and S are required to fit the spectrum, while Fe appears to be underabundant. This suggests that the interstellar medium in the starburst nuclear region has been enriched by the ejecta of type-II supernova explosions. Moreover, a high abundance of C and a high C/O abundance ratio can be the effect of radiatively-driven winds from metal-rich Wolf-Rayet stars with $M \gtrsim 40 M_{\odot}$ (Gustafsson et al. 1999). Both effects are likely to be present in the nuclear region.

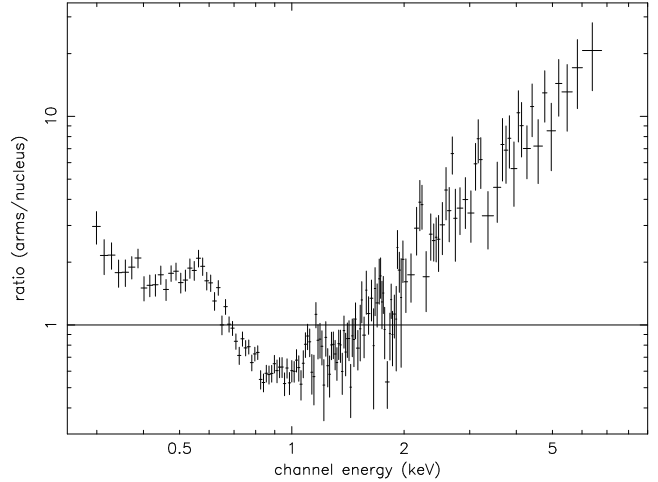


Figure 5. The ratio between the unresolved emission in the spiral arms and the best-fit model to the unresolved emission in the nuclear region shows that: a) the thermal component in the spiral arms is cooler ($T \approx 0.31$ keV in the arms, $T \approx 0.58$ keV in the nucleus); b) a power-law component dominates the spiral-arm emission at energies $\gtrsim 1$ keV. The two spectra have been normalised to the same number of counts.

Strong unresolved emission is also detected along the arms. It is well fitted by a thermal component at $kT \approx 0.3$ keV and a power-law component ($\Gamma \approx 1.5$) dominating at energies $\gtrsim 1$ keV. A study of this higher-energy component and a comparison with the Galactic Ridge emission will be presented in a work now in preparation.

ACKNOWLEDGEMENTS

We thank Stefan Immler, Roy Kilgard, Miriam Krauss, Casey Law, Oak-Young Park, Elena Pian, Allyn Tennant and Daniel Wang for helpful discussions and suggestions.

REFERENCES

- Côté, S., Freeman, K. C., Carignan, C. & Quinn, P. 1997, *AJ*, 114, 1313
 Giacconi, R., et al. 2001, *ApJ*, 551, 624
 Gustafsson, B., Karlsson, T., Olsson, E., Edvardsson, B. & Ryde, N. 1999, *A&A*, 342, 426
 Immler, S., Volger, A., Ehle, M. & Pietsch, W. 1999, *A&A*, 352, 415
 Okada, K., Mitsuda, K. & Dotani, T. 1997, *PASJ*, 49, 653
 Sandage, A. & Tammann, G. A. 1987, *A revised Shapley-Ames Catalog of Bright Galaxies*, 2nd ed., (Carnegie Institution of Washington Publication: Washington)
 Schlegel, D. J., Finkbeiner, D. P. & Davis, M. 1998, *ApJ*, 500, 525
 Soria, R., Wu, K., 2002, *A&A*, in press (astro-ph/0201059)
 Tennant, A. F., Wu, K., Ghosh, K. K., Kolodziejczak, J. J. & Swartz, D. A. 2001, *ApJ*, 549, L43
 Trinchieri, G., Fabbiano, G. & Palumbo, G. G. C. 1985, *ApJ*, 290, 96
 de Vaucouleurs, G. 1979, *AJ*, 84, 1270

de Vaucouleurs, G., de Vaucouleurs, A., Corwin, H., Jr., Buta,
R., Paturel, G. & Fouque, P. 1991, Third Reference Cata-
logue of Bright Galaxies (Springer: New York)
Wu, K. 2001, PASA, 18, 443